Magnetic Resonance Imaging with Laser Polarized ^{129}Xe

Scott D. Swanson, Matthew S. Rosen, Bernard W. Agranoff, Kevin P. Coulter, Robert C. Welsh, Timothy E. Chupp

University of Michigan
Ann Arbor, Michigan 48109

Abstract. Magentic Resonance Imaging with laser-polarized ^{129}Xe can be utilized to trace blood flow and perfusion in tissue for a variety of biomedical applications. Polarized xenon gas intoduced in to the lungs dissolves in the blood and is transported to organs such as the brain where it accumulates in the tissue. Spectroscopic studies combined with imaging have been used to produce brain images of ^{129}Xe in the rat head. This work establishes that nuclear polarization produced in the gas phases survives transport to the brain where it may be imaged. Increases in polarization and delivered volume of ^{129}Xe will allow clinical measurements of regional blood flow.

I INTRODUCTION

Advances in laser polarization of ^{3}He and ^{129}Xe, motivated in large part by polarized target experiments, has led to significant activity in NMR and MRI of laser-polarized noble gases for medical applications. This is because the NMR signal per atom for laser polarized gases is sufficient to make up for the small concentrations compared to protons in tissue used in conventional NMR and MRI. Gas phase images of ^{3}He or ^{129}Xe have been obtained from excised mouse lungs [1], in vivo guinea pig lungs [2], and humans [3–5]. Gas phase imaging may provide detailed, tomographic information about lung ventilation as dicussed in other contributions in this session. With xenon, it is possible to create tissue phase images in addition to gas phase images. Xenon dissolves in blood [6], accumulates in the brain [7], and may be treated as a freely diffusible tracer in vivo [8]. These properties have allowed xenon to be used by SPECT [9] and CT [10] to measure regional cerebral blood flow (rCBF) by analyzing uptake and washout curves of xenon in the brain [11]. A number of spectroscopic studies have also been performed of ^{129}Xe dissolved in blood in vitro [12,13] and in blood and/or tissue in vivo [14]. Given high levels of

CP421, *Polarized Gas Targets and Polarized Beams:* Seventh International Workshop
edited by Roy J. Holt and Michael A. Miller
© 1998 The American Institute of Physics 1/56396-700-6/98/$15.00

nuclear polarization and desirable biological properties for measuring rCBF, we set out to determine the feasibility of using laser-polarized ^{129}Xe as a magnetic tracer to measure rCBF and perfusion in other tissue such as the heart. For this method to be successful, the nuclear polarization created in the gas phase must survive transport from the lungs, into the blood, through the heart, and into the brain.

II TECHNIQUES

We have constructed an optical pumping and polarized ^{129}Xe delivery system shown in figure 1.

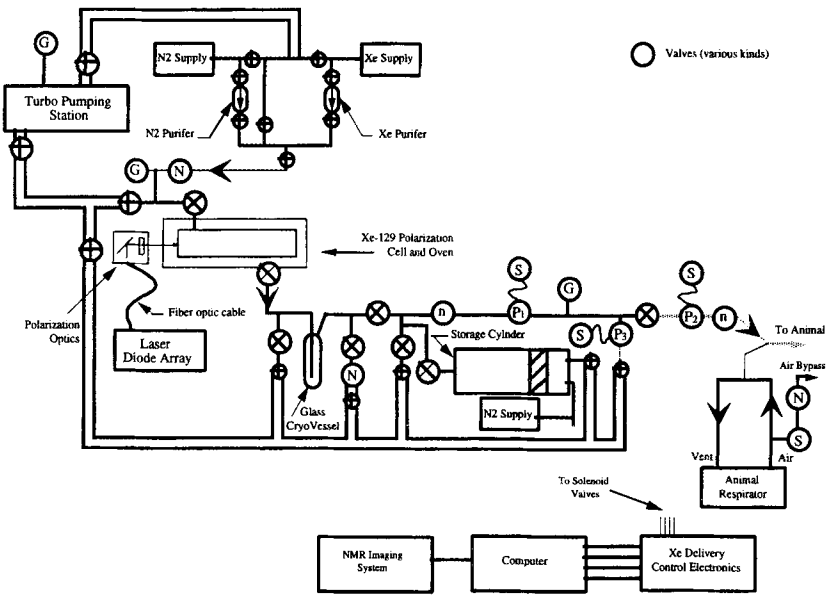

Figure 1. Schematic diagram of laser polarization and delivery system for ^{129}Xe MRI. The optical pumping takes place in the fringing field of the 2 T MRI magnet. The ^{129}Xe is polarized in the pumping chamber, transfered to a storage volume and delivered to the animal in single breath doses.

High nuclear polarization of noble gases is achieved by spin-exchange with optically-pumped Rb [15–19]. The results shown below were obtained with ^{129}Xe polarized to approximately 3.5% in an optical pumping cell containing 1700 Torr of xenon (26.4% ^{129}Xe) and 200 Torr of N2 to quench radiation trapping. The optical pumping cell, a 75 cc Pyrex cylinder with hemispherical end windows, is coated with octadecyltrichlorosilane to reduce depolarizing ^{129}Xe-wall interactions [20]. High vacuum techniques are essential to minimize contaminants such as paramagnetic O_2 which decrease nuclear spin T1 and limit absolute polarization [21]. Two Teflon valves mounted on the cell allow

evacuation, filling, and delivery of the gases. Optimum density of rubidium vapor was achieved by heating the cell to 95°C. Two laser diode arrays (Optopower, Tucson, AZ), each providing at 15 Watts of continuous laser light, were used for optical pumping. Commercial availability of these high powered, efficient, GaAlAs laser diode arrays at the Rb D1 wavelength has made a tremendous impact on the field [22]. The entire apparatus including lasers, optics, valves, heating and cooling, and transport tubing lies in the peripheral magnetic field of the 2 T solenoid magnet with the optical pumping cell collinear with the solenoid axis. Typical polarization times in these studies were 10 to 15 minutes, producing sufficient amounts of polarized ^{129}Xe to ventilate a 250 gm rat for 40 to 50 seconds. NMR and MRI data were obtained with a three-turn, doubly-tuned proton-^{129}Xe surface coil [23] with 3.5 cm diameter. Excitation and response of the surface coil were determined by phantom studies to be sufficiently homogenous over the region of interest.

Spectra and images obtained with rats are shown in figures 2 and 3. The ^{129}Xe spectrum shown in figure 2 was obtained with 64 averages and a 50 microsecond RF pulse with an estimated tip angle of 10°.

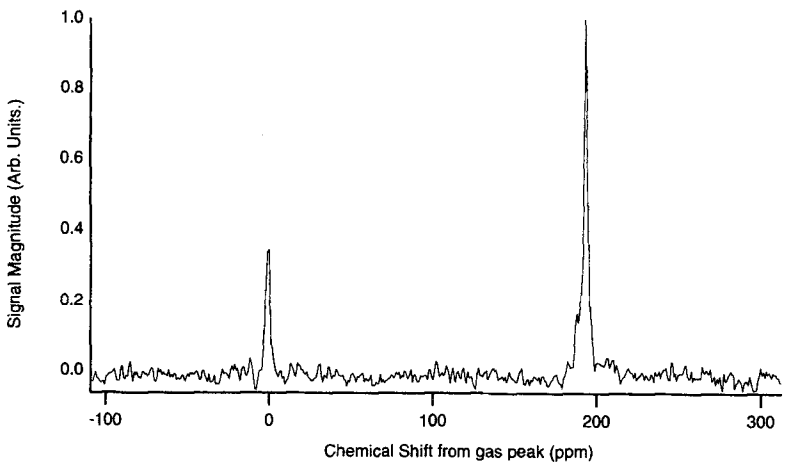

Figure 2. Magnetic resonance spectra of ^{129}Xe obtained with the head coil. The blood tissue resonance is near 200 ppm. The small gas peak near 0 ppm is due to gas in the intubation tube, sinuses, and mouth.

The ^{129}Xe tissue image shown in Fig. 3 was acquired with a 2D chemical shift imaging pulse sequence that uses phase encoding to separate the blood/tissue spectral component from the gas phase peak [24] The sequence produced a slice thickness of 10 mm, a field-of-view of 50 mm x 50 mm, a block size of 256 complex points and an estimated flip angle of 20°. The total imaging time was 73 s. The 256 x 16 x 16 CSI dataset was zero filled along both phase-encode

dimensions to produce a final matrix size of 256 x 32 x 32. These data were Fourier transformed along each dimension with the magnitude of the spectrum calculated in each voxel. A Lorentzian function was fitted to the ^{129}Xe tissue phase resonance in each of the 1024 spectra and the amplitudes of the fit used to generate the ^{129}Xe image shown in Fig. 2A. The proton image shown in Fig. 2C was acquired with a conventional spin-echo pulse sequence with a slice thickness of 10 mm, a field of view of 50 x 50 mm. Precise registration of the ^{129}Xe image with respect to the proton image is important to interpretation of information contained in the ^{129}Xe image.

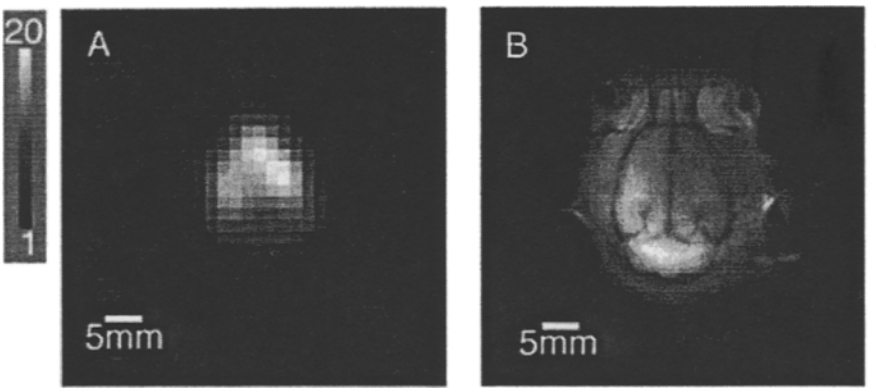

Figure 3. Magnetic resonance images of the rat head with A) ^{129}Xe and B) proton imaging.

III RESULTS AND DISCUSSION

The NMR spectrum acquired from the rat head (figure 2) has two resolvable resonances: a small gas resonance due to ^{129}Xe in the intubation tube and a single, dominant, blood/tissue resonance at 194.5 ppm relative to the gas peak. The NMR image of ^{129}Xe in the head is presented in figure 3A. The gray scale for indicates signal amplitude relative to the RMS noise fluctuations of the background (SNR). The maximum SNR for a voxel is approximately 20. The blood/tissue resonance seen in Fig. 2 is assigned to ^{129}Xe in brain tissue based on the following argument: the rat brain cerebral blood volume is relatively low ($\approx$ 5%); cerebral blood flow very high ($\approx$ 1.0 ml/g per min.); and the partition coefficient between brain and blood is approximately 1.0 [7]. Since brain tissue has a much larger capacity for xenon than the brain blood and since xenon will freely diffuse into brain tissue, the NMR signal observed will be dominated by ^{129}Xe in the brain. This reasoning is supported by the image of ^{129}Xe in the rat head (Figs. 2A and B) which shows that the ^{129}Xe

signal is localized to the brain and not seen the surrounding fat or muscle. ^{129}Xe magnetization observed in the rat brain is not uniform. ^{129}Xe signal in the cerebellum is less than the signal in the cerebrum. The signal difference could be due to partial volume effects or to lower blood flow in the cerebellum than in the cerebrum. Sakurada *et al.* found blood flow for cerebellar gray matter similar to or somewhat lower than that of cerebral gray matter [?]. In addition, inhalation of xenon has been shown to increase cerebral but not cerebellar regional blood flow [28]. Figures 3A and B also show that the two hemispheres of the cerebrum are marginally separated in the ^{129}Xe image.

The time dependence of ^{129}Xe magnetizatio in the brain has been studied with a model of ^{129}Xe magnetization uptake in the brain [25,26]. The data and results are shown in figure 4, where time dependence from the model are shown for several values of ^{129}Xe T1. We use this to estimate the T1 relaxation time of polarized ^{129} in the brain, indicating that T1 is approximately 30 seconds or greater.

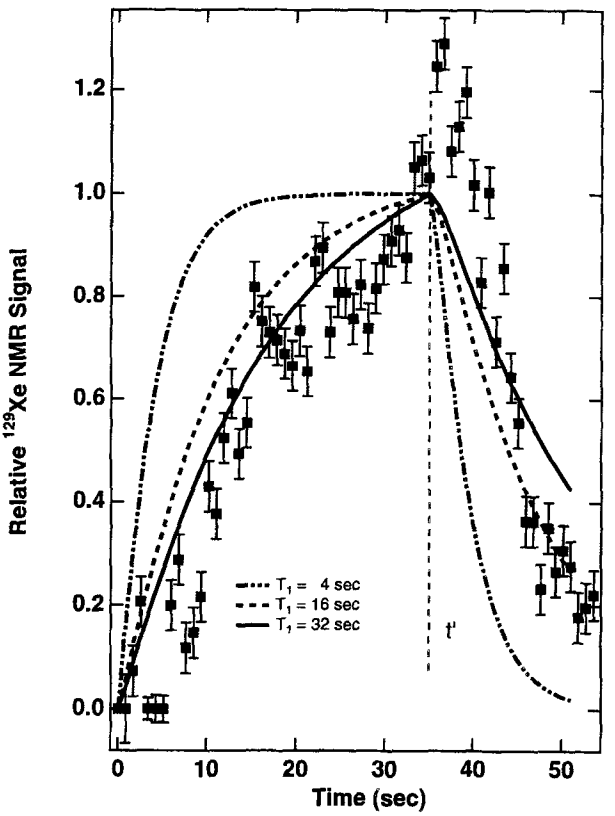

Figure 4. Uptake of blood/tissue spectral component in the head. The solid lines are model results for several T1 ^{129}Xe relaxation times.

IV CONCLUSION

The work described here is part of the large world-wide effort to use laser polarized noble gases for biomedical NMR and MRI. This effort has engaged many physicists with expertise in polarized targetry. Our work represents the first use of laser-polarized ^{129}Xe for NMR spectroscopy and imaging of the brain, in vivo. The importance of laser-polarized ^{129}Xe in studies of regional brain activation by measurement of rCBF follows from the limitations of currently employed techniques and the complementary use of radioactive and magnetic tracers.

In order to extend these techniques to humans, greater volumes and polarizations of laser-polarized ^{129}Xe will be required. In our current apparatus, we accumulate and store laser-polarized ^{129}Xe by freezing [29] for long-duration animal and human rCBF experiments. We also mix oxygen and reduce the Xe concentration to approximately 30% to avoid anoxia and anesthetic effects of xenon. Signal loss must be compensated for by increases in polarization, or the use of expensive isotopically enriched ^{129}Xe.

Though useful experiments can be performed with ^{129}Xe polarization of 1 - 10%, higher polarization will be necessary to increase the spatial and/or temporal resoulution of ^{129}Xe brain imaging. Polarizations of 50% or more have been achieved in small volumes with more suitable lasers. Advances in laser technology and the polarization delivery system should yield significantly higher ^{129}Xe polarization in the future.

Laser-polarized ^{129}Xe imaging need not be limited to the brain. Since xenon dissolves in blood and tissue, combined gas phase/tissue phase pulmonary imaging of ^{129}Xe may provide tomographic ventilation/perfusion information not available with ^{3}He. In addition, measurement of cardiac perfusion may be feasible with laser-polarized ^{129}Xe if the blood and tissue components resonate at different frequencies. Finally, since the polarization produced by laser optical pumping is magnetic field independent, it is interesting to consider of MRI at low fields (0.1 T or less). Low field techniques may provide less expensive, lighter, and more compact scanners for medical purposes.

V ACKNOWLEDGMENT

We gratefully acknowledge essential discussions with Drs. Paul Carson, Kirk Frey, Robert Koeppe, and Martin Prince and Philip Sherman for assistance with animal care and use. This work was supported in part by NSF and the University of Michigan's Office of Vice President for Research, Frontiers in Neuroscience Fund, the Department of Physics, and the Department of Radiology.

REFERENCES

1. M.S. Albert, G.D. Cates, B. Driehuys, W.Happer, B Saam, C.S. Springer, Jr., and A. Wishnia, *Nature*, **370**, 199-201 (1994).
2. R.D. Black, H.L. Middleton, G.D. Cates, G.P. Cofer, B. Driehuys, W. Happer, L.W. Hedlund, G.A. Johnson, M.D. Shattuck, and J.C. Swartz, *Radiology*, **199**, 867-70 (1996).
3. J.R. MacFall, H.C. Charles, R.D. Black, H. Middleton, J.C. Swartz, B. Saam, B. Driehuys, C. Erickson, W. Happer, G.D. Cates, G.A. Johnson, and C.E. Ravin. *Radiology*, **200**, 553-8 (1996).
4. H.U. Kauczor, D. Hofmann, K.F. Kreitner, H. Nilgens, R. Surkau, W. Heil, A. Potthast, M.V. Knopp, E.W. Otten, M. Thelen, *Radiology*, **201**, 564-8 (1996).
5. J.P. Mugler, III, B. Driehuys, J.R.Brookeman, G.D. Cates, S.S. Berr, R.G. Bryant, T.M. Daniel, E.E. de Lange, C.J. Erickson, W. Happer, D.P. Hinton, T. Maier, B.T. Saam, K.L. Sauer, M.E. Wagshul, *Proc., ISMRM, 5th Annual Meeting, Vancouver*,2113 (1997).
6. S.Y. Yeh, R.E. Peterson,. *Appl. Physiol.*, **20**, 1041-7 (1965).
7. R.Y.Z. Chen, F.C. Fan, S. Kim, K.M. Jan, S. Usami, S. Chien, *J. Appl. Physiol.*, **49**, 178-181 (1980).
8. S.S. Kety, *Pharmacol. Rev.*, **3**, 1-41 (1951).
9. N.A. Lassen, in *"Cerebral Metabolism and Neural Function"* (J.V. Passonneau, R.A.Hawkins, W.D. Lust, F.A. Welsh, Eds.) pp. 144-150, Williams and Wilkins, Baltimore, (1980).
10. K. Nambu, R. Suzuki, K. Hirakawa. *Radiology*, **195**, 53-57 (1995).
11. S.S. Kety, C.F. Schmidt, *Am. J. Physiol.*, **143**, 53 (1945).
12. A. Bifone, Y.Q. Song, R. Seydoux, R.E. Taylor, B.M. Goodson, T. Pietrass, T.F. Budinger, G. Navon, A. Pines,*Proc. Natl. Acad. Sci.*, **93**, 12932-6, (1996).
13. M. Albert, V.D. Schepkin, T.F. Budinger,*J. Comput. Assist. Tomogr.*, **19**, 975-978 (1995).
14. M.E. Wagshul, T.M. Button, H.F. Li Z. Liang, C.S. Springer, K. Zhong, and A. Wishnia, *Magn. Reson. Med.*, **36**, 183 - 91 (1996).
15. T. G. Walker, W. Happer, *Rev. Mod. Phys.*, **69**, 629 - 42 (1997).
16. T.E. Chupp, K.P. Coulter, *Phys. Rev. Lett.*, **55**, 1074-1077 (1985).
17. X. Zeng, Z. Wu, T. Call, E. Miron, D. Schreiber, W. Happer, *Phys. Rev. A*, **31**, 260 - 78 (1985).
18. T.E. Chupp, M. Wagshul, K.P. Coulter, A.B. McDonald, W. Happer,*Phys. Rev. C*, **36**, 2244-2241 (1987).
19. G.D. Cates, R.J. Fitzgerald, A.S. Barton, P. Bogorad, M. Gatzke, N.R. Newbury, B. Saam, *Phys Rev. A*, **45**, 4631-9 (1992).
20. E.R. Oteiza, *Ph.D. Dissertation*, Harvard University (1992).
21. B. Saam, W. Happer, H. Middleton, *Phys. Rev. A*, **52**, 862-865 (1995).
22. M.E. Wagshul, T.E. Chupp, *Phys. Rev. A*, **40**, 4447-4454 (1989).
23. V. Cross, R. Hester, J. Waugh, *Rev. Sci. Instrum.*, **47**, 1486-1488 (1976).
24. T.R. Brown, B.M. Kincaid, K. Ugurbil, *Proc. Natl. Adac. Sci. U.S.A.*, **79**, 3523-3526 (1982).

25. S. Peled *et al. Mag. Res. Med.* **37**, 809-815 (1997).
26. K.P. Coulter *et al.* private communication – to be published (1997).
27. O. Sakurada, C. Kennedy, J. Jehle, J.D. Brown, G.L. Carbin, L. Sokoloff, *Am. J. Physiol.*, **234**, H59-H66 (1978).
28. L. Junck, V. Dhawan, H.T. Thaler, D.A. Rottenberg, *J. Cereb. Blood Flow Metab.*, **5**, 126-132 (1985).
29. G.D. Cates, D.R. Benton, M. Gatzke, W. Happer, K.C. Hasson, N.R. Newbury, *Phys. Rev. Lett.*, **65**, 2591-2594 (1990).